Karlsruher Institut für Technologie

Averaged stress intensity factors for semi-elliptical surface cracks

K.G. Schell, C. Bucharsky, G. Rizzi, T. Fett

KIT SCIENTIFIC WORKING PAPERS 169

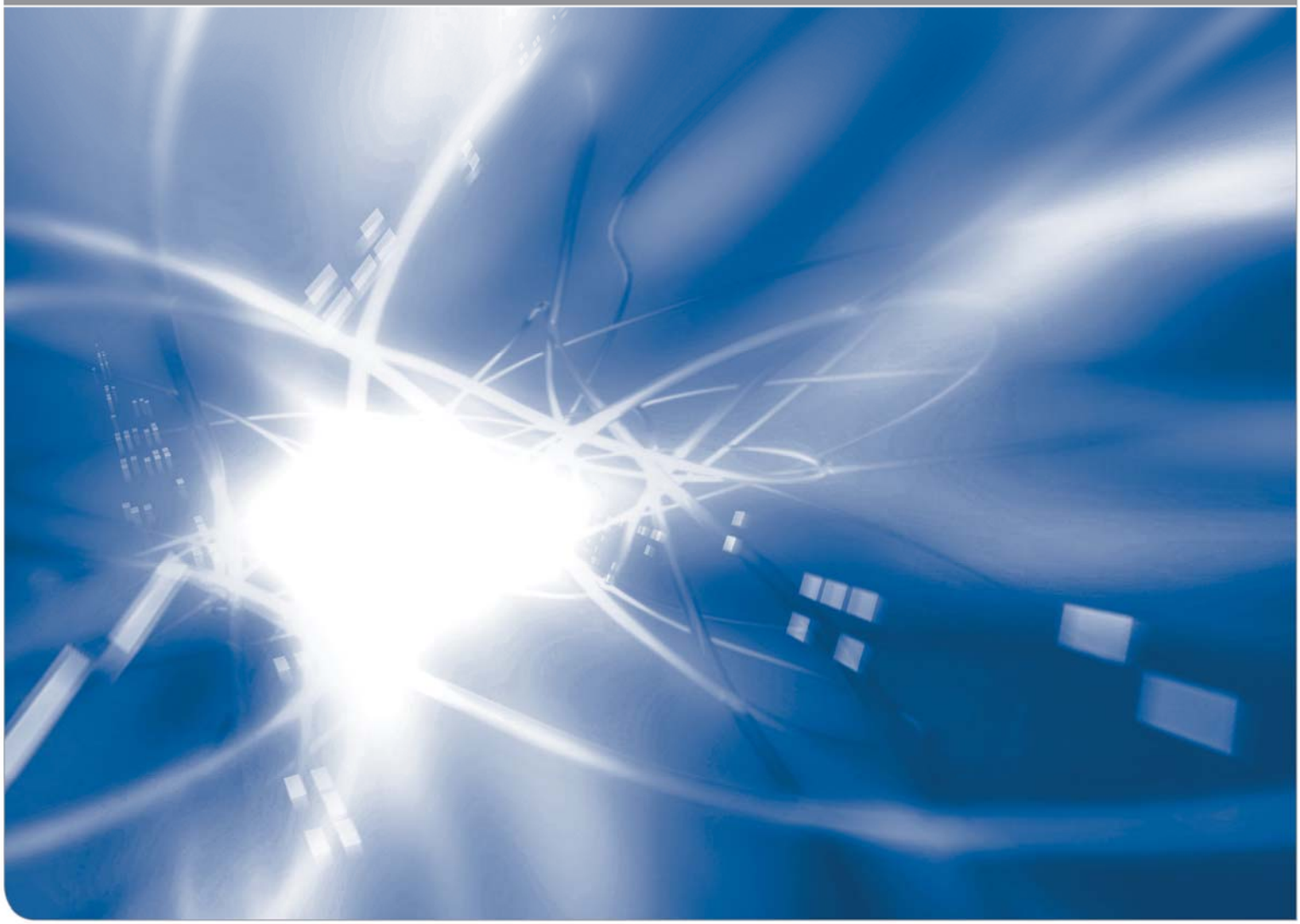

KIT – Universität des Landes Baden-Württemberg und nationales Forschungszentrum in der Helmholtz-Gemeinschaft

IAM Institute for Applied Materials

Impressum

Karlsruher Institut für Technologie (KIT)
www.kit.edu

2021

ISSN: 2194-1629

Abstract

The measurement of material resistance against crack propagation is mostly performed with (in principle) one-dimensional cracks as usual for standard test specimens as for instance DCB (Double Cantilever Beam) specimens. Such a crack exhibits a constant stress intensity factor along the crack front that allows simple computations of crack extension.

In the case of 2-dimensional cracks, e.g. semi-elliptical surface cracks, the calculation of strength and service life under subcritical crack growth is considerably more complicated. The main reason for this is the fact that the stress intensity factor changes along the crack front.

In this report, averaged *K*-factors for virtual crack propagation in both axial directions of the semi-ellipse are determined. For this purpose, virtual crack area increments according to Cruse and Besuner are used.

The stress intensity factors for the deepest point of the crack and the surface terminating points are given by polynomials obtained via curve fitting of the numerical results.

In addition, the averaged *K*-factors under concentrated forces were estimated.

Contents

1. Local stress intensity factors by Newman and Raju

Cracks generated on glass surfaces during machining are responsible for strength and lifetimes of mechanically loaded specimens. The same holds for artificially introduced indentation cracks. The semi-elliptical cross section of such a surface crack is shown schematically in Fig. 1a. The crack depth is denoted as *a* and crack width as *2c*. The parametric angle along the crack front is φ and the stress acting normal on the crack plane is σ. The deepest point of the crack is generally denoted as point (A) and the intersection points at the surface as (B).

For the computation of local stress intensity factors $K(\varphi)$ under a tensile stress σ, the well established relation of Newman and Raju [1] may be used. This relation reads

$$K = \sigma Y \sqrt{a} \tag{1}$$

with the geometric function modified in [2]:

$$Y = \frac{\sqrt{\pi}}{\mathbf{E}(1-a^2/c^2)}(1+0.122\,\mathrm{erfc}[0.69\tfrac{a}{c}])\,[1+0.1(1-\sin\varphi)^2]\left[\left(\frac{a}{c}\right)^2\cos^2\varphi+\sin^2\varphi\right]^{1/4} \tag{2}$$

where **E** stands for the complete elliptic integral of second kind. Figure 1b shows the geometric function $Y(\varphi)$ for several aspect ratios *a*/*c*.

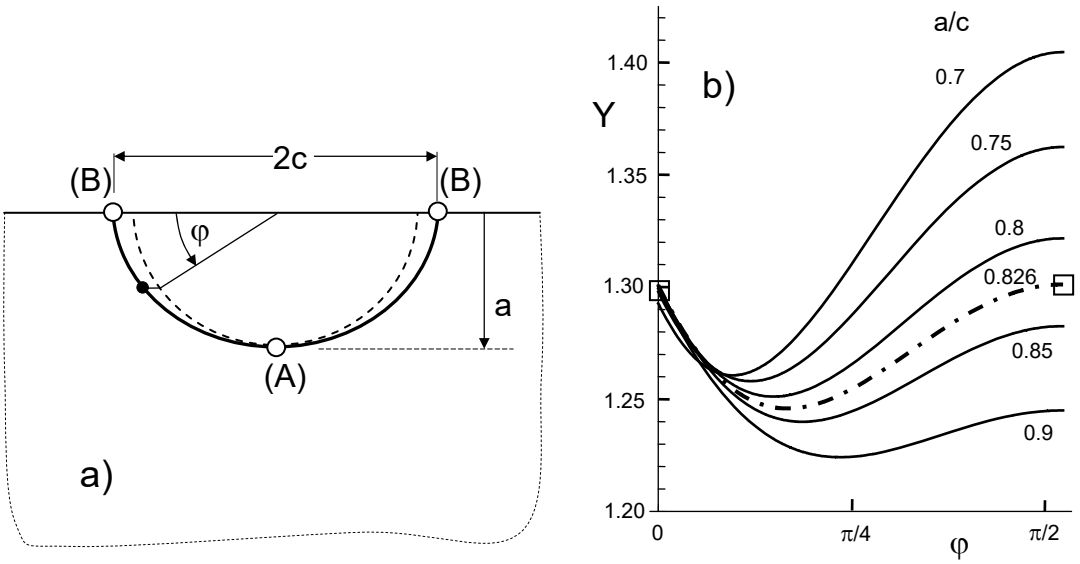

Fig. 1 a) Geometry of a semi-elliptical surface crack normal to the applied stress, b) geometric function along the crack front for several aspect ratios *a*/*c*, dash-dotted line: curve for which $Y_A=Y_B$ (represented by squares).

The geometric function at the points (B) and (A), i.e. for φ=0 and φ=π, is shown in Fig. 2a. The stress intensity factors at these points are represented in Fig. 2b. For aspect

ratios of $a/c<0.826$, the stress intensity factor is at (A) higher than at points (B). At $a/c>0.826$, the reverse applies, $K_A<K_B$.

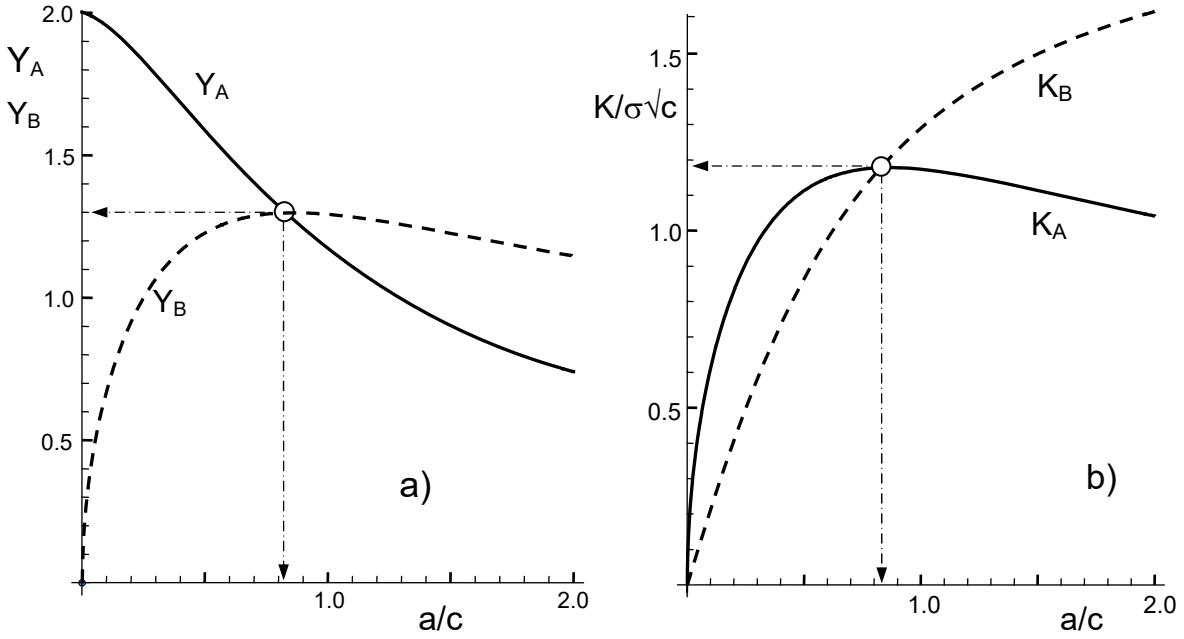

Fig. 2 Local stress intensity factors: a) geometric function at the deepest (A) and the surface points (B) of a semi-elliptical crack, b) related stress intensity factors K_A and K_B. Circles indicate $Y_A=Y_B$ and $K_A=K_B$.

2 Averaged stress intensity factors according to Cruse and Besuner

2.1 Averaged stress intensity factors

Figure 1b implies that:

- There exists no aspect ratio for a semi-ellipse that yields a constant stress intensity factor along the crack front.
- Even for the aspect ratio of $a/c=0.826$ for which the local stress intensity factors at the surface and the deepest point of the semi-ellipse are identical, the stress intensity factor shows a significant variation with the angle φ. This fact causes problems in describing crack propagation. Problems are obvious even in the simplest case of crack extension, namely, stable crack growth at $K=K_{Ic}$. By load application to a semi-elliptic crack of $a/c=0.826$, the critical stress intensity factor is at first reached at the surface and the deepest points. These regions can extend but the regions at which $K(\varphi)<K(0°,90°)$ must stay behind a semi-ellipse (Fig. 3). Already after the first infinitesimally small step of crack extension, the crack geometry must deviate from a semi-ellipse and, consequently, the semi-ellipse solution can no longer be applied to this now slightly irregular crack shape. This makes evident that stable and subcritical crack growth prediction on the basis of

local stress intensity factors is not simply possible. From observation of the crack shape during stable and fatigue crack propagation it could be concluded that cracks propagated as semi-ellipses although local stress intensity factors did not allow this. An irregular shape to be expected from the local variation of the stress intensity factors was not detectable. A way out of this dilemma was proposed very early by Cruse and Besuner [3] as will be considered here.

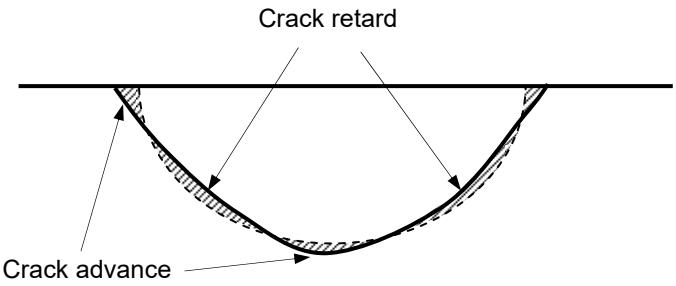

Fig. 3 Prediction of a semi-elliptical crack extension by stable or subcritical crack propagation, schematic, dashed front: original crack, solid front: Front, developed during crack propagation.

A simple fracture mechanics tool to compute the shape of semi-elliptical surface cracks is the computation of so-called averaged stress intensity factors.
The definition of the average stress intensity factor $\overline{K}$ according to Cruse and Besuner [3,4,9] is

$$\overline{K} = \sqrt{\frac{1}{\Delta S}\int_{(\Delta S)} K^2 d(\Delta S)} \tag{3}$$

Two independent virtual crack changes that preserve the semi-elliptical crack shape were proposed by Cruse and Besuner [3], namely, crack depth increment Δa with width c kept constant

$$\Delta S_A = \tfrac{1}{2}\pi c \Delta a\ ,\ d(\Delta S_A) = c\Delta a \sin^2\varphi\, d\varphi \tag{4}$$

or crack width increment Δc with depth $a = \text{const}$

$$\Delta S_B = \tfrac{1}{2}\pi a \Delta c\ ,\ d(\Delta S_B) = a\Delta c \cos^2\varphi\, d\varphi \tag{5}$$

as illustrated in Fig. 4 by the hatched areas.
It should be emphasized that the Cruse-Besuner approach for the computation of averaged stress intensity factors was examined intensively in the eighties and early nineties. Only a few papers may be mentioned in this context which shows that the method is applicable to various types of cracks. The theoretical and experimental analyses on simple semi-elliptical surface cracks in plates and bars (see e.g. [7]) were extended to

more complicated crack problems as for instance almond- and sickle-shaped cracks in rods [5,6] and corner cracks [7]. In [8] the procedure was successfully applied to indentation cracks in glass. Problems of the accuracy were discussed in [9].
The use of this type of stress intensity factors allowed very good predictions for the development of the crack shape in tension and bending and correct predictions of crack growth rates in fatigue tests. In the following considerations stress intensity factors defined by eqs.(3) to (5) will be addressed.

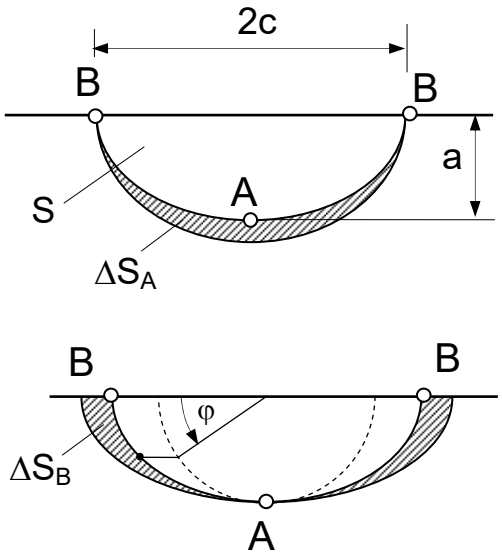

Fig. 4 Virtual crack extensions according to Cruse and Besuner [3].

2.2 Numerical results for remote tension

By introducing the local stress intensity factor $K(\varphi)$, eqs.(1) and (2) into (3), the virtual crack extensions according to (4) and (5) resulted in the averaged geometric functions, Fig. 5a, and the averaged stress intensity factors, Fig. 5b.
By curve fitting, we obtained approximate relations for the averaged geometric functions at points (A) and (B) defined by

$$\overline{K}_{A,B} = \sigma \overline{Y}_{A,B} \sqrt{a} \tag{6}$$

At the deepest point (A) it is

$$\overline{Y}_A = 0.476 + 1.14 \exp\left[-0.58 \frac{a}{c} \right] + 0.238 \exp\left(-1.309 \frac{a^2}{c^2} \right) \tag{7}$$

and at the surface points (B)

$$\overline{Y}_B = 0.82 \exp\left[-0.0145 \frac{a}{c} \right] + 0.5066 \exp\left(-0.1924 \frac{a^2}{c^2} \right) \tag{8}$$

Particularly noteworthy is the fact that in the range $0.75<a/c<3$ the stress intensity factor K_A is almost constant (indicated by the dash-dotted horizontal line in Fig. 5b). Therefore, it can be written

$$\overline{K}_A = \sigma 1.18\sqrt{c} \tag{9}$$

The curves of the K-factors defined according to eq.(3) intersect at about $a/c \approx 0.85$. For aspect ratios of $a/c<0.85$, the averaged stress intensity factor is at (A) higher than at points (B).

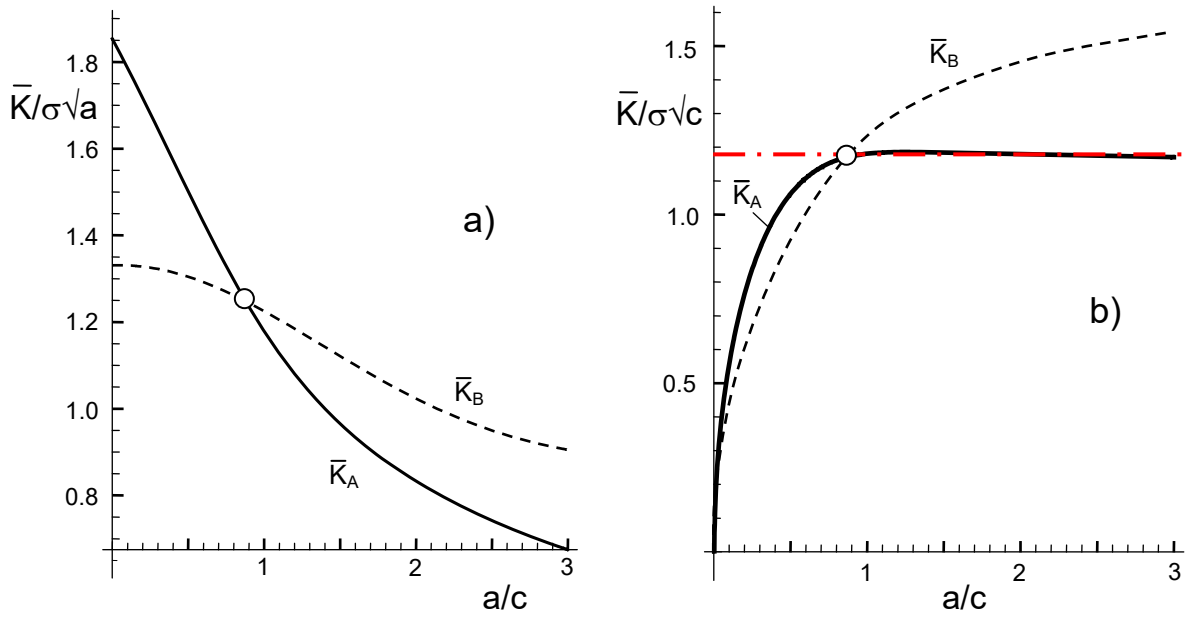

Fig. 5 Averaged stress intensity factors in two equivalent representations, a) normalized on the crack depth a, b) normalized on the crack width c.

3 Surface cracks under concentrated force

3.1 Surface crack caused during machining

Figure 6 shows a crack that has been created under a strongly localized contact between a grain of a grinding wheel and the glass surface.

The result of such a contact may be described by a crack-like damage similar to the cracks obtained by Vickers indentation tests. Beneath the contact area of indenter and glass surface, a residual stress zone of depth ρ remains even after unloading. Plastically deformed glass and material pressed between the crack flanks act as a wedge and open the crack. The result is a positive stress intensity factor $K_r>0$. If the size of the residually stressed zone is sufficiently small compared to the crack size, the stresses distributed over a cross-section of radius ρ, may be replaced by a single point force P at the crack mouth that acts perpendicularly on the crack plane. The stress intensity factors for such a crack-face loading were fitted in [2].

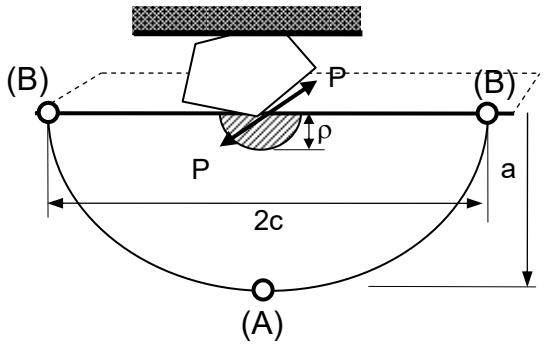

Fig. 6 Geometric data of an indentation crack: Indentation process by a single grain of the grinding wheel, resulting in a semi-elliptical surface crack of depth a and width $2c$.

3.2 Semi-elliptical surface crack and embedded elliptical crack

Averaged stress intensity factors for the semi-elliptical crack under a point force are available in Chapter F4.2 of [10]. These results are plotted in Fig. 7a for the limited range of $0.7 \le a/c \le 1$ expressed in [10] by

$$\overline{K}_{A,B} = \frac{2P_{semi}}{(\pi a)^{3/2}} \overline{F}_{A,B} = \frac{2P_{semi}}{(\pi c)^{3/2}} \left(\frac{c}{a}\right)^{3/2} \overline{F}_{A,B} \tag{10}$$

with the geometric functions for the limited region of $0.7 \le a/c \le 1$:

$$\overline{F}_A = 0.018 + 2.886\frac{a}{c} - 2.602\left(\frac{a}{c}\right)^2 + 0.732\left(\frac{a}{c}\right)^3 \tag{11}$$

$$\overline{F}_B = -0.175 + 0.714\frac{a}{c} + 1.357\left(\frac{a}{c}\right)^2 - 0.565\left(\frac{a}{c}\right)^3 \tag{12}$$

Numerical results for local stress intensity factors on embedded elliptical cracks subjected by point forces were reported by Atroshchenko [11] in Figs. 3.16 and 3.18. We fitted these data in [2] and expressed the numerical solutions by

$$K_A \frac{(\pi c)^{3/2}}{P_{ell}} \cong \frac{3}{a/c + (a/c)^2 + (a/c)^3} \tag{13}$$

for point (A) and

$$K_B \frac{(\pi c)^{3/2}}{P_{ell}} \cong 1.275 \frac{2.479(a/c)^2 + 1.157(a/c)^3}{1 + 2.479(a/c)^2 + 1.157(a/c)^3} \tag{14}$$

for point (B). The black dashed curves are the local stress intensity factors for the embedded elliptical crack. In a fit procedure, we used the results for the internal crack

as the general trend and fitted the data of the range $0.7 \le a/c \le 1.0$ satisfying trivial limit condition for $a/c \to \infty$: $K_A \to 0$, $dK_B/d(a/c) \to 0$.

The crack-opening forces for the elliptical crack P_{ell} and for the surface crack P_{semi} differ by a factor of 2: $P_{ell}=2P_{semi}$. The reason is that by cutting the internal elliptical crack into two "surface cracks", the load is also halved.

As approximate relations for the averaged stress intensity factors we suggest for the extended region $0.7 \le a/c \le 3$.

$$\overline{K}_A \frac{(\pi c)^{3/2}}{2P_{semi}} \cong \frac{3.74}{\frac{a}{c}+\left(\frac{a}{c}\right)^2+\left(\frac{a}{c}\right)^3}\left(1-\exp\left[-1.76\frac{a}{c}\right]\right) \tag{15}$$

for point (A), and

$$\overline{K}_B \frac{(\pi c)^{3/2}}{2P_{semi}} \cong 1.22+0.144\exp\left[-5.06\left(\frac{a}{c}-0.775\right)^2\right] \tag{16}$$

for point (B), both solutions introduced by the dashed red curves.

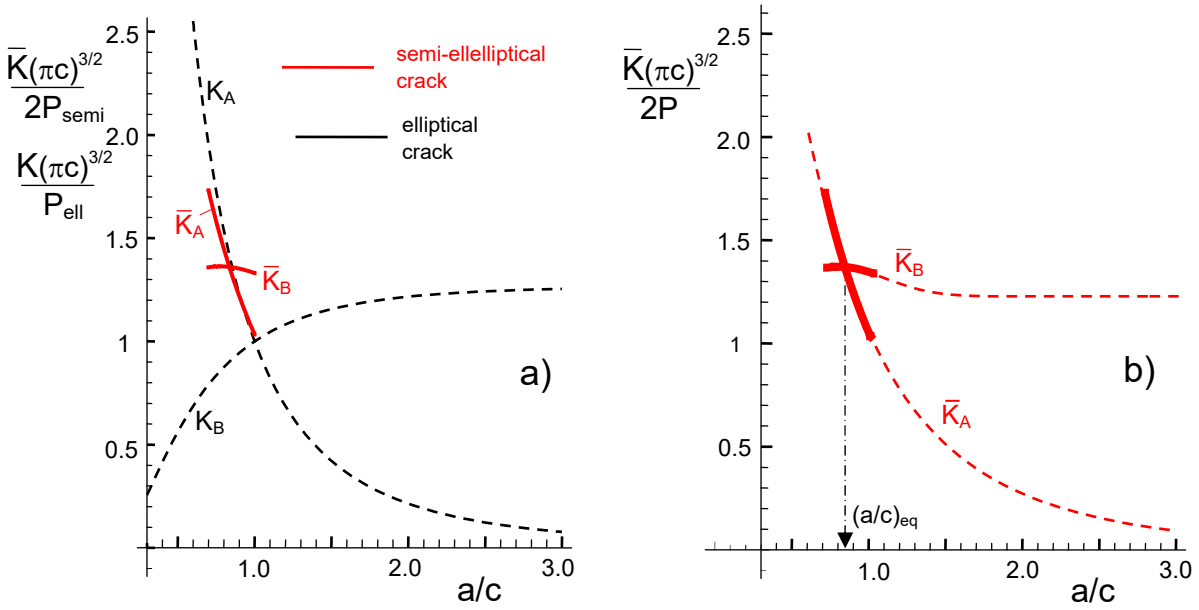

Fig. 7 a) Averaged stress intensity factors for surface cracks [10] under concentrated force, (red curve segments), compared with the (dashed black curves), local stress intensity factors for the embedded crack (black) [2], b) extrapolation of the data from [10] for $0.7 \le a/c \le 3$ indicated by the dashed red curves. Arrow: equilibrium aspect ratio $(a/c)_{eq} \cong 0.84$.

References

1 Newman, J.C., Raju, I.S., An empirical stress intensity factor equation for the surface crack, Engng. Fract. Mech. **15**(1981), 185-192.

2 T. Fett, K.G. Schell, C. Bucharsky, Indentation events during surface machining - Compilation of local stress intensity factors, Scientific Working Papers **163**, 2020, ISSN: 2194-1629, Karlsruhe, KIT

3 Cruse, T.A., Besuner, P.M., Residual life prediction for surface cracks in complex structural details, J. of Aircraft **12**(1975), 369-375.

4 Fett, C. Mattheck, D. Munz, On the accuracy of the Cruse-Besuner weight function approximation for semi-elliptical surface cracks, Int. Journ. of Fracture **40**(1989), 307-313

5 Keer, L.M., Farris, T.N., Lee, J.C., Knoop and Vickers indentation in ceramics analyzed as a three-dimensional fracture, J. Am. Ceram. Soc. **69**(1986), 392-96.

6 M. Caspers, C. Mattheck, Weighted averaged stress intensity factors for circular-fronted cracks in cylindrical bars, Fatigue Fract. Engng. Mater. Struct. **9**(1987), 329-341.

7 Varfolomeyev, I.V., Vainshtok, V.A., Krasowsky, A.Y., Prediction of part-through crack growth under cyclic loading, Engng. Fract. Mech. **40**(1991), 1007-1022.

8 T. Fett, K. Keller, D. Munz, Determination of subcritical crack growth on glass in water from lifetime measurements on Knoop cracked specimens, J. Mat. Sci. **23**(1988), 798-803

9 T. Fett, D. Munz, Stress intensity factors and weight functions, Computational Mechanics Publications, 1997, Southampton.

10 T. Fett, Stress Intensity Factors, T-Stresses, Weight Functions, Supplement Volume, IKM **55**, KIT Scientific Publishing, 2009.

11 E. Atroshchenko, Stress intensity factors for elliptical and semi-elliptical cracks subjected to an arbitrary mode I loading, Thesis, 2010, University of Waterloo, Ontario, Canada.

KIT Scientific Working Papers
ISSN 2194-1629

www.kit.edu